improve this performance toward quantum limits. Higher frequencies also appear to be accessible to this promising device.

ACKNOWLEDGMENT

Stimulating discussions with P. T. Parrish, H. E. Rowe, and K. S. Yngvesson are gratefully acknowledged. Special thanks are due to J. R. Tucker for making his theory available to us before publication, and for helpful discussions and to R. E. Miller for technical assistance.

REFERENCES

[1] P. L. Richards, T.-M. Shen, R. E. Harris, and F. L. Lloyd, *Appl. Phys. Lett.*, vol 34, pp. 345–347, 1979.
[2] G. J. Dolan, T. G. Phillips, and D. P. Woody, *Appl. Phys. Lett.*, vol. 34, pp. 347–349, 1979.
[3] S. Rudner and T. Claeson, *Appl. Phys. Lett.*, vol. 34, pp. 711–713, 1979.
[4] S. M. Farris, *Appl. Phys. Lett.*, vol. 36, pp. 1005–1007, 1978.
[5] J. R. Tucker, *IEEE J. Quantum Electronics*, vol. QE-15, pp. 1234–1258, 1979.
[6] M. H. Cohen, L. M. Falicov, and J. C. Phillips, *Phys. Rev. Lett.*, vol. 8, pp. 316–318, 1962.
[7] H. C. Torrey and C. A. Whitmer, *Crystal Rectifiers*. New York: McGraw-Hill, 1948.
[8] J. R. Tucker, *Appl. Phys. Lett.*, vol. 36, pp. 477–479, 1980.
[9] T.-M. Shen, P. L. Richards, R. E. Harris, and F. L. Lloyd, *Appl. Phys. Lett.*, vol. 36, pp. 777–779, 1980.
[10] R. A. Linke, M. V. Schneider, and A. Y. Cho, *IEEE Trans. Microwave Theory Tech.*, vol. MTT-26, pp. 935–938, 1978.
[11] T. G. Phillips and K. B. Jefferts, *Rev. Sci. Instr.*, vol. 44, 1009–1012, 1973.
[12] W. C. Scott, *Appl. Phys. Lett.*, vol. 17, pp. 166–169, 1972.
[13] B. N. Taylor and E. Burstein, *Phys. Rev. Lett.*, vol. 10, pp. 14–17, 1963.
[14] K. Kleinman, *Phys. Rev.*, vol. 132, pp. 2484–2489, 1963.
[15] A. H. Dayem and R. J. Martin, *Phys. Rev. Lett.*, vol. 8, pp. 246–248, 1962.
[16] P. K. Tien and J. P. Gordon, *Phys. Rev.*, vol. 129, pp.647–651, 1963.
[17] D. A. Fleri and L. D. Cohen, *IEEE Trans. Microwave Theory Tech.*, vol. MTT-21, pp. 39–43, 1973.
[18] A. R. Kerr, *IEEE Trans. Microwave Theory Tech.*, vol. MTT-23, 828–831, 1975.

# Mode Analysis in Multimode Waveguides Using Voltage Traveling Wave Ratios

DAVID S. STONE

*Abstract*—**The voltage traveling wave ratio (VTWR) equations are discussed in general and the specific case of guided traveling waves in multimode circular waveguides is addressed in detail. An experimental technique for measuring VTWR's is described and sample experimental results are analyzed. Measurements of the VTWR's can be easily related to the fractions of total power propagating in each waveguide mode. This information may be used, for example, to examine the mode conversion properties of multimode waveguide components.**

## I. INTRODUCTION

MULTIMODE transmission lines, with their virtue of very low insertion loss, have been considered by many authors for long distance communications applications [1]. Recent advances in high average power millimeter wave sources, such as the gyrotron [2]–[4], have revived interest in the study of multimode waveguides to handle power densities which would be prohibitively high in single mode systems.

The ratio of the maximum and minimum values of the beating wave electric fields of any two modes propagating in a multimode guide may, by analogy to the well-established vernacular of the single mode waveguide, be denoted the voltage traveling wave ratio (VTWR) for the two modes in question. In general, the VTWR's will be a function of position in the plane normal to the direction of propagation in the guide. Measurements of the VTWR's can be easily related to the mode power, or the fractions of total power propagating in each waveguide mode. This information may be used to: 1) characterize the operating mode output of a high power source with multimode output such as a gyrotron; 2) analyze the mode conversion properties of overmoded waveguide components; 3) determine the optimum locations along the line for lossy obstructions; and 4) allow impedance matching (induced destructive interference of one or more unwanted modes) [5].

Manuscript received July 24, 1980; revised September 30, 1980. This work was supported by the United States Department of Energy and the Union Carbide Corporation under Contract W-7405-eng-26.

The author is with Varian Associates, Inc., Palo Alto, CA 94303.

0018-9480/81/0200-0091$00.75 ©1981 IEEE

In the following section we mathematically define the voltage traveling wave ratio. The beat pattern resulting from the presence of a large but finite number of guided traveling modes is analyzed in Section III and related to the mode power fractions. The special case of two circular electric modes propagating in cylindrical waveguide is treated in Section IV and this analysis is applied to a set of VTWR measurements in Section V.

## II. Voltage Traveling Wave Ratio

Consider the superposition of two plane waves with complex amplitudes $A_n$ and $A_m$ traveling in the positive $z$ direction. We may write the resultant wave amplitude as

$$C(z)=|A_n|e^{-ik_nz-i\phi_n}+|A_m|e^{-ik_mz-i\phi_m} \tag{1}$$

where

$$\phi_{n,m}\equiv\arctan\left\{\frac{\operatorname{Im}\langle A_{n,m}\rangle}{\operatorname{Re}\langle A_{n,m}\rangle}\right\} \tag{2}$$

and $k_{n,m}$ are the propagation constants or wavenumbers. We are interested in cases where such a resultant wave, or beat pattern, is measured by a detector sensitive to the quantity

$$|C(z)|^2=|A_n|^2+|A_m|^2 +2|A_n||A_m|\cos\{(k_n-k_m)z+(\phi_n-\phi_m)\}. \tag{3}$$

We can identify the beat wavenumber $K_{nm}\equiv|k_n-k_m|/2$. The beat wavelength is $\lambda_{nm}\equiv 2\pi/K_{nm}$. We may eliminate the beat phase, $(\phi_n-\phi_m)$, by suitable choice of origin in $z$. Solving for the ratio of the maximum and minimum values of $|C(z)|$ we define the *voltage traveling wave ratio* (VTWR)

$$\text{VTWR}\equiv\frac{|C(z)|_{\max}}{|C(z)|_{\min}}=\frac{||A_n|+|A_m||}{||A_n|-|A_m||}=\pm\frac{|A_n|+|A_m|}{|A_n|\mp|A_m|},$$

$$\text{upper sign: } |A_n|>|A_m|, \qquad \text{lower sign: } |A_n|<|A_m| \tag{4}$$

where the value of the VTWR can range from unity to infinity. Turning this expression around we find the ratio

$$\frac{|A_m|^2}{|A_n|^2}=\left(\frac{\text{VTWR}\mp 1}{\text{VTWR}\pm 1}\right)^2, \qquad \text{upper sign: } |A_n|>|A_m|,$$

$$\text{lower sign: } |A_n|<|A_m|. \tag{5}$$

Equation (5) relates a measurable quantity, the VTWR for modes $n$ and $m$, to the ratio of traveling plane wave amplitudes. The proper choice of signs in (5) will be discussed in more detail in Sections III and IV.

## III. Arbitrary Cross-Sectional Waveguide, Many Modes Present

We wish to deduce the fractions $|a_n|^2$ of the total transmission line power contained in each waveguide mode from the measured beat wave pattern $|C(\boldsymbol{r},z)|^2$. The multimode transmission line is uniform in the direction of propagation but may have any arbitrary cross section. The superposition of many modes traveling in the positive $z$ direction gives the measured resultant wave amplitude

$$C(\boldsymbol{r},z)=\sqrt{C_0}\sum_n a_nR_n(\boldsymbol{r})e^{-ik_nz} \tag{6}$$

where the propagation wavenumbers $k_n$ are real and constant, the sum is performed over a finite number of modes, and the constant $C_0$ represents the sensitivity of the detector. The $a_n$'s are normalized according to

$$\sum_n|a_n|^2=1. \tag{7}$$

In the plane (denoted by $\boldsymbol{r}$) orthogonal to the $z$ axis, the amplitude of each mode has a spatial dependence $R_n(\boldsymbol{r})$. As the dimensions of the waveguide cross section are known, the $R_n$'s are known, orthogonal, and normalized

$$\int d^2\boldsymbol{r}R_n(\boldsymbol{r})R_m^*(\boldsymbol{r})=\delta_{n,m}. \tag{8}$$

The integral in $\boldsymbol{r}$ is taken over the entire waveguide cross section. The "square-law" detector measures the quantity

$$|C(\boldsymbol{r},z)|^2=C_0\sum_{n,m}a_na_m^*R_n(\boldsymbol{r})R_m^*(\boldsymbol{r})e^{-i(k_n-k_m)z}. \tag{9}$$

Taking the Fourier transform of both sides of (9)

$$\frac{1}{2\pi}\int_{-\infty}^{\infty}dz\,e^{ikz}|C(\boldsymbol{r},z)|^2 =C_0\sum_{n,m}a_na_m^*R_n(\boldsymbol{r})R_m^*(\boldsymbol{r})\delta(k-(k_n-k_m)). \tag{10}$$

To find the total intensity of each spectral line in $k$-space we operate on (10) with $\lim_{\epsilon\to 0}\int_{K-\epsilon}^{K+\epsilon}dk$, where $K\equiv k_{n'}-k_{m'}$ with $n'$ and $m'$ undetermined, and we find

$$\lim_{\epsilon\to 0}\frac{1}{\pi}\int_{-\infty}^{\infty}dz|C(\boldsymbol{r},z)|^2\cdot\frac{\sin\epsilon z}{z}e^{iKz} =C_0\sum_{n,m}a_na_m^*R_n(\boldsymbol{r})R_m^*(\boldsymbol{r})D_{nm}(K) \tag{11}$$

where

$$D_{nm}(K)=\delta_{n',n}\delta_{m',m}, \qquad n\neq m$$
$$=\delta_{n',m'}, \qquad n=m. \tag{12}$$

We have assumed that there exists no $(n',m')$ for which $k_{n'}-k_{m'}=k_n-k_m$. Thus, we exclude the simultaneous presence of two or more modes degenerate in $k_n$. For $n=m$, (11) and (12) give

$$C_0=\lim_{\epsilon\to 0}\frac{1}{\pi}\int_{-\infty}^{\infty}dz\frac{\sin\epsilon z}{z}\int d^2\boldsymbol{r}|C(\boldsymbol{r},z)|^2 \tag{13}$$

where we have imposed (7) and (8). For $n\neq m$ we find

$$C_0a_na_m^*R_n(\boldsymbol{r})R_m^*(\boldsymbol{r}) =\lim_{\epsilon\to 0}\frac{1}{\pi}\int_{-\infty}^{\infty}\frac{\sin\epsilon z}{z}e^{i(k_n-k_m)z}|C(\boldsymbol{r},z)|^2. \tag{14}$$

Taking the absolute square of both sides, dividing through by $|R_m(\boldsymbol{r})|^2$, and summing $\sum_{m\neq n}$, we solve the resulting

TABLE I
RADIAL DEPENDENCE OF BEAT PHASE FOR CIRCULAR ELECTRIC MODES

| $TE_{on}$ Radial Dependence: $J_1\left(\frac{x_n r}{a}\right)$ | $TE_{om}$ Radial Dependence: $J_1\left(\frac{x_m r}{a}\right)$ | $\pi(\sigma_n(r)-\sigma_m(r))$ |
|---|---|---|
| > 0 | > 0 | 0 |
| < 0 | > 0 | $+\pi$ |
| > 0 | < 0 | $-\pi$ |
| < 0 | < 0 | 0 |

quadratic equation for the *mode power fraction*:

$$|a_n|^2 = \frac{1}{2} \pm \frac{1}{2}\sqrt{1 - \frac{4\sum_{m\neq n}|R_m(r)|^{-2}\left|\int_{-L/2}^{L/2} dz e^{i(k_n-k_m)z}|C(r,z)|^2\right|^2}{|R_n(r)|^2\left|\int_{-L/2}^{L/2} dz \int d^2r |C(r,z)|^2\right|^2}}. \tag{15}$$

The limit in $\epsilon$ and the limits on the integral in $z$ have been discarded and replaced with a finite integration interval $L$ over which the beat pattern is measured. This treatment is valid as long as

$$L \gtrsim \frac{1}{2}\langle \lambda_{nm} \rangle \tag{16}$$

where the brackets $\langle\ \rangle$ indicate the longest beat wavelength of interest in the system.

Equation (15) is the desired result. It states that the mode power fraction for the $n$th mode is deduced by: 1) measuring the beat wave pattern at some point $\boldsymbol{r}$ over a length $L$ which satisfies (16); 2) transforming the beat pattern into beat wavenumber space; 3) summing transform contributions from all beat wavenumbers after weighting each term by the proper $\boldsymbol{r}$ dependence; and 4) normalizing the sum over $m\neq n$ to the $\boldsymbol{r}$ dependence of the $n$th mode and the volume integral of the beat pattern. The ambiguity in sign which occurs in (15) has been observed in the simple case (5), and results from the fact that the square law detector rectifies the transmission line signal and thus ignores necessary phase information. In practice, one resolves this ambiguity by performing measurements at two different points $\boldsymbol{r}$ and then choosing the sign which gives a result independent of $\boldsymbol{r}$. This point will be discussed further in Section IV.

## IV. CYLINDRICAL WAVEGUIDES—TWO CIRCULAR ELECTRIC MODES PRESENT

The coefficients in (17) have been normalized as required by (7) and (8). The roots of $J_1(x)=0$ are denoted as $x_n (n \geq 1)$ and $r$ and $a$ are the radial coordinate and waveguide wall radius. Taking the absolute square of (17) we have

$$C(r,z) = \frac{\sqrt{2}\,|a_n|}{|J_0(x_n)|}J_1\left(\frac{x_n r}{a}\right)e^{-ik_n z - i\phi_n} \frac{\sqrt{2}\,|a_m|}{|J_0(x_m)|}J_1\left(\frac{x_m r}{a}\right)e^{-ik_m z - i\phi_m}. \tag{17}$$

The coefficients in (17) have been normalized as required by (7) and (8). The roots of $J_1(x)=0$ are denoted as $x_n (n \geq 1)$ and $r$ and $a$ are the radial coordinate and waveguide wall radius. Taking the absolute square of (17) we have

$$\begin{aligned}|C(r,z)|^2 = {} & \frac{2|a_n|^2\left|J_1\left(\frac{x_n r}{a}\right)\right|^2}{|J_0(x_n)|^2} + \frac{2|a_m|^2\left|J_1\left(\frac{x_m r}{a}\right)\right|^2}{|J_0(x_m)|^2} \\ & + \frac{4|a_n||a_m|\left|J_1\left(\frac{x_n r}{a}\right)\right|\left|J_1\left(\frac{x_m r}{a}\right)\right|}{|J_0(x_n)||J_0(x_m)|} \\ & \cdot \cos\{(k_n-k_m)z + (\phi_n-\phi_m) \\ & + \pi(\sigma_n(r)-\sigma_m(r))\}. \end{aligned} \tag{18}$$

The term $\pi(\sigma_n(r)-\sigma_m(r))$ results from the convention for positive definite wave coefficients adopted in (1) and may be easily evaluated using Table I. Equation (18) also contains the familiar beat wavenumber $K_{nm} \equiv |k_n - k_m|/2$. For modes of interest here we may compute the beat wavelengths

$$\begin{aligned}\lambda_{nm} \equiv \frac{2\pi}{K_{nm}} &= \frac{2\lambda}{\left|\sqrt{1-\frac{\lambda^2 x_n^2}{4\pi^2 a^2}} - \sqrt{1-\frac{\lambda^2 x_m^2}{4\pi^2 a^2}}\right|} \\ &\cong \frac{16\pi^2 a^2}{\lambda|x_n^2 - x_m^2|}, \qquad \text{for } \frac{\lambda^2 x_{n,m}^2}{4\pi^2 a^2} \ll 1 \end{aligned} \tag{19}$$

where $\lambda$ is the free space wavelength. Using (5) and (17) we find the *mode power ratio*

$$\frac{|a_m|^2}{|a_n|^2} = G_{nm}(r)\left(\frac{\text{VTWR}\ (r) \mp 1}{\text{VTWR}\ (r) \pm 1}\right)^2 \tag{20}$$

TABLE II
CHOICE OF SIGN IN (20)

| Case | Calculated Quantity | Measured Quantity | Proper Sign |
|---|---|---|---|
| 1 | $G_{nm}(r_1) > G_{nm}(r_2)$ | $VTWR(r_1) > VTWR(r_2)$ | Lower Sign |
| 2 | $G_{nm}(r_1) > G_{nm}(r_2)$ | $VTWR(r_1) < VTWR(r_2)$ | Upper Sign |
| 3 | $G_{nm}(r_1) < G_{nm}(r_2)$ | $VTWR(r_1) > VTWR(r_2)$ | Upper Sign |
| 4 | $G_{nm}(r_1) < G_{nm}(r_2)$ | $VTWR(r_1) < VTWR(r_2)$ | Lower Sign |

with

$$G_{nm}(r) \equiv \frac{|J_0(x_m)|^2 \left|J_1\left(\frac{x_n r}{a}\right)\right|^2}{|J_0(x_n)|^2 \left|J_1\left(\frac{x_m r}{a}\right)\right|^2} \quad \text{and} \quad G_{nm}(r) = G_{mn}^{-1}(r).$$

Of course, we could also have arrived at (20) directly from (17) by employing the definition (4) and the general formula (15).

To resolve the ambiguity in signs in (20) we make VTWR measurements at two positions, $r_1$ and $r_2$, and then require

$$G_{nm}(r_1)\left(\frac{\mathrm{VTWR}\,(r_1)\mp 1}{\mathrm{VTWR}\,(r_1)\pm 1}\right)^2 = G_{nm}(r_2)\left(\frac{\mathrm{VTWR}\,(r_2)\mp 1}{\mathrm{VTWR}\,(r_2)\pm 1}\right)^2. \tag{21}$$

After some algebra, (21) leads to four inequalities

$$\mp \mathrm{VTWR}\,(r_1)\mathrm{VTWR}\,(r_2)[\mathrm{VTWR}\,(r_2) - \mathrm{VTWR}\,(r_1)] \pm [\mathrm{VTWR}\,(r_2) - \mathrm{VTWR}\,(r_1)] \gtrless 0. \tag{22}$$

The four corresponding solutions are summarized in Table II. To choose the proper sign in (20) we must measure and compare the values of VTWR $(r_1)$ and VTWR $(r_2)$ and calculate and compare the coefficients $G_{nm}(r_1)$ and $G_{nm}(r_2)$. Table II will then indicate the proper choice of sign.

## V. VTWR Measurements

We now present an example of the application of VTWR measurements. The experiments were carried out using a traveling wave indicator of novel design (see Fig. 1) which can be scanned in $r$, $\theta$, and $z$ with resolutions of $dr \sim 0.2a$, $rd\theta \sim 0.2a$, and $dz \approx \lambda/2$. The traveling waves were detected with a polarimetric probe adjusted to pick up signals proportional to the square of the azimuthal wave electric field $|E_\theta|^2$. VTWR measurements were performed in 2.5-in diameter waveguide at the downstream end of a complex but axisymmetric overmoded waveguide structure, the output/collector section of a Varian VGA-8000 gyrotron. A $TE_{02}$ wave at 28 GHz was launched into the structure from the upstream end. The quantity $|E_\theta|^2$ was measured for $r = -a$ to $+a$ at a number of axial positions $z$, as shown in Fig. 2.

It is apparent from Fig. 2 that the launched $TE_{02}$ wave has been partially converted into other circular electric modes. For the moment we ignore the presence of the $TE_{03}$ mode by plotting $|E_\theta(z)|^2$ versus $z$ at two different

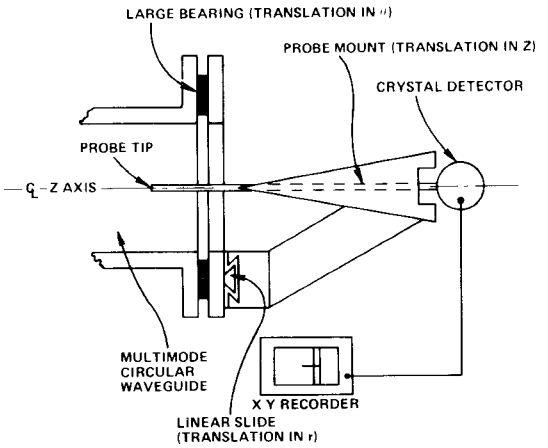


Fig. 1. Schematic diagram of a novel traveling wave indicator used for measurement of VTWR's in multimode cylindrical waveguides. The instrument is capable of remotely controlled scanning in radius and azimuth and may be scanned manually in the axial direction.

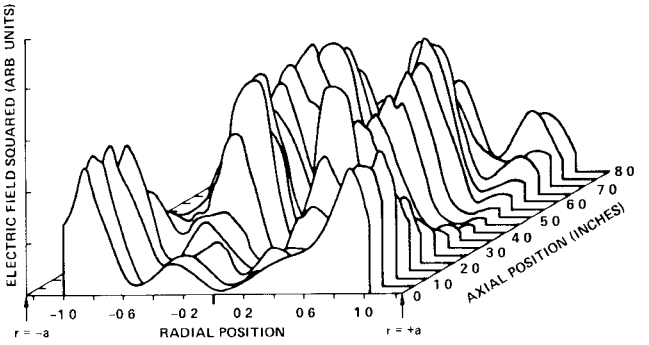


Fig. 2. Measured beat pattern, as seen in cold test, of the mode output of the Varian VGA-8000 gyrotron. The traveling wave indicator signal, which is proportional to $|E_\theta|^2$, is plotted in arbitrary units versus radius and axial position.

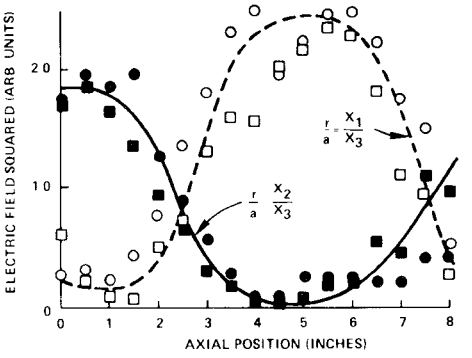


Fig. 3. Measured beat pattern, as seen in cold test, of the mode output of the Varian VGA-8000 gyrotron. The traveling wave indicator signal, which is proportional to $|E_\theta|^2$, is plotted in arbitrary units versus axial position at two different radial positions on both sides of the waveguide: $r = +x_1 a/x_3$ (open circles), $r = -x_1 a/x_3$ (open squares), $r = +x_2 a/x_3$ (solid circles), and $r = -x_2 a/x_3$ (solid squares). The VTWR's have been determined by drawing roughly sinusoidal curves through the data and then using (4).

radial positions for which the $TE_{03}$ is identically zero, $r = x_1 a/x_3, x_2 a/x_3$. The results are shown in Fig. 3. The beat wave pattern of the $TE_{01}$ and $TE_{02}$ modes is clearly evident. The beat wavelength measured (~16 in) is close

TABLE III
MODE POWER FRACTIONS AT OUTPUT OF VGA-8000 GYROTRON

| Mode | Measured Mode Power Fraction (%) |
|---|---|
| $TE_{01}$ | 27 ± 5 |
| $TE_{02}$ | 63 ± 5 |
| $TE_{03}$ | 10 ± 5 |
| All other modes | 0 + 5 - 0 |
| | Total 100% |

to that predicted by (18). Furthermore, the beat phase jumps by $\sim\pi$ rad from its value at $r=x_1a/x_3$ to its value at $r=x_2a/x_3$ as predicted in Table I.

We apply the VTWR definition (4) to the fitted curves in Fig. 3 and find

$$\mathrm{VTWR}\left(\frac{x_1a}{x_3}\right)=3.9$$

$$\mathrm{VTWR}\left(\frac{x_2a}{x_3}\right)=6.9$$

while we calculate

$$G_{12}\left(\frac{x_1a}{x_3}\right)=0.796$$

$$G_{12}\left(\frac{x_2a}{x_3}\right)=1.258.$$

We now employ (20) with the lower set of signs (as dictated by Table II) and take the mean of the mode power ratio measurements made at $r=x_1a/x_3, x_2a/x_3$. A similar analysis may be performed on the beat pattern between the $TE_{01}$ and $TE_{03}$ modes, by setting $r=x_1a/x_2$. The measured mode power fractions are summarized in Table III, where we have required the proper normalization (7).

## VI. CONCLUSIONS

We have described a technique for measurement of the voltage traveling wave ratios in multimode waveguides for the wavelength regime $d/L\lesssim\lambda/d\lesssim 0.2$, where $d$ is the characteristic size of the waveguide cross section and $L$ is the axial length over which the multimode beat pattern must be observed (16). Such measurements provide information necessary for design of multimode waveguide components and integration of such components into complex multimode systems. In illustration, we have analyzed cold test measurements of the mode conversion of a $TE_{02}$ mode by a series of axisymmetric mismatches. We have also addressed the general problem of measuring mode conversion properties of severe nonaxisymmetric mismatches. The task is handled by measuring the beat pattern over an axial length $L$ and Fourier transforming the data into beat wave number space.

## ACKNOWLEDGMENT

The author is indebted to N. Taylor and Dr. H. Derfler for many useful discussions.

## REFERENCES

[1] R. Hecken and A. Anuff, "on the optimum design of tapered waveguide transitions," *IEEE Trans. Microwave Theory Tech.*, vol. MTT-21, pp. 374–380, June 1973.

[2] J. F. Shively, P. Ferguson, H. R. Jory, J. Moran, and R. S. Symons, "Recent advances in gyrotrons," in *1980 IEEE-MTT Int. Microwave Symp. Dig.*, (Washington, DC), May 1980, pp. 99–101.

[3] H. Jory, C. Conner, S. Evans, J. Moran, W. Sayer, D. Stone, R. Symons, and G. Thomas, "Development program for a 200 kW CW, 28 GHz gyroklystron," Varian Associates, Quarterly Rep. no. 16, Rep. no. ORNL/Sub-01617/16, Mar. 1980.

[4] H. Jory, S. Evans, J. Moran, J. Shively, D. Stone, and G. Thomas, "Pulsed and CW gyrotron oscillators for plasma heating," presented at 2nd Joint Grenoble-Varenna Int. Symp. Heating in Toroidal Plasmas, (Como, Italy), Sept. 3–12, 1980.

[5] L. Solymar, "Monotonic multi-section tapers for overmoded circular waveguides," *Proc. IEE*, vol. 106, pt. B, suppl. no. 13, pp. 121–128, Jan. 1959.